Acta Biotheor
DOI 10.1007/s10441-013-9177-5

REGULAR ARTICLE

Intrinsic Feedbacks in MAPK Signaling Cascades Lead to Bistability and Oscillations

Jacques-Alexandre Sepulchre · Alejandra C. Ventura

Received: 4 December 2012 / Accepted: 22 January 2013

Abstract Previous studies have demonstrated that double phosphorylation of a protein can lead to bistability if some conditions are fulfilled. It was also shown that the signaling behavior of a covalent modification cycle can be quantitatively and, more importantly, qualitatively modified when this cycle is coupled to a signaling pathway as opposed to being isolated. This property was named retroactivity. These two results are studied together in this paper showing the existence of interesting phenomena—oscillations and bistability—in signaling cascades possessing at least one stage with a double-phosphorylation cycle as in MAPK cascades.

Keywords Signaling cascade · MAPK · Retroactivity

1 Introduction

Covalent modification cycles are one of the major intracellular signaling mechanisms, both in prokaryotic and eukaryotic organisms (Alberts et al. 2001). Signaling pathways are made up of chains or cascades of such cycles, in which the activated protein in one cycle promotes the activation of the protein in the next one. In this

J.-A. Sepulchre (✉)
Institut Non Linéaire de Nice, UMR 7335 CNRS, University of Nice Sophia Antipolis, 1361 route des Lucioles, 06560 Valbonne, France
e-mail: jacques-alexandre.sepulchre@inln.cnrs.fr

A. C. Ventura
Instituto de Fisiología, Biología Molecular y Neurociencias, CONICET, Buenos Aires, Argentina
e-mail: alejvent@fbmc.fcen.uba.ar

A. C. Ventura
Departamento de Fisiología, Biología Molecular y Celular, Facultad de Ciencias Exactas y Naturales, Universidad de Buenos Aires, Ciudad Universitaria, Pabellón 2, 2 piso, C1428EHA Buenos Aires, Argentina

Published online: 12 February 2013

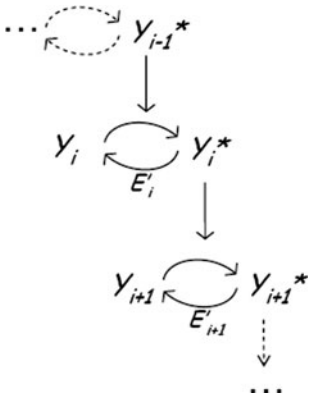

Fig. 1 Schematic representation of a cascade of covalent modification cycles. The *ith* cycle is composed of two states of the same protein: the inactive and the active states, labeled Y_i and Y_i^*, respectively. In each step, the activation is catalyzed by the activated product of the previous step. The deactivation is mediated by another enzyme, E_i'

way, an input signal injected at one end of the pathway can propagate traveling through its building-blocks to elicit one or more effects at a downstream location. The advantages of these cascades in signal transduction are multiple: a reaction cascade may amplify a weak signal, it may accelerate the speed of signaling, can steepen the profile of a graded input as it is propagated, filter out noise in signal reception, introduce time delay, and allow alternative entry points for differential regulation (Bluthgen et al. 2006; Ortega et al. 2002; Thattai and van Oudenaarden 2002).

The scheme in Fig. 1 is usually employed to represent a cascade. From a systemic point of view, a cascade is a system composed of units, the output of which is successively an input to the next unit. This kind of schematic representation implicitly conveys the idea that a signaling cascade is only a feed-forward chain in which signal transmission is analogous to a domino effect (Murray and Kirschner 1989; Gonze and Goldbeter 2001): the information flows in only one direction. Adding explicit connections linking a particular level with an upstream location has been the way bidirectional propagation has been explained until recently.

The model we proposed in (Ventura et al. 2008) shows that an intrinsic negative feedback emerges naturally, exerted between each cycle and its predecessor. Similar results were reported by Del Vecchio et al. (2008) giving the name of *retroactivity* to the phenomenon. Our work showed that, because of that intrinsic negative feedback, each unit of the cascade is actually coupled not only to the following one but also to the previous one, meaning that a cascade can naturally exhibit bidirectional propagation without invoking extra re-wiring. Therefore, the schematic representation in Fig. 1 can be misleading. Our theoretical/computational results were later on experimentally validated (Ventura et al. 2010; Kim et al. 2011; Jiang et al. 2011) and further characterized (Ossareh et al. 2011; Wynn et al. 2011).

In (Ventura et al. 2008) we considered mainly the case of single-covalent modification cascades with no much details devoted to the case of double-covalent modification cascades. We could show that due to the mentioned negative feedback, a cascade of single-covalent modification cycles displays damped temporal oscillations under constant stimulation and, most important, propagates perturbations both forwards and backwards. However, the case comprising double-phosphorylation is

important in practise as it concerns the mitogen activated protein kinase (MAPK) cascade, which is widely involved in eukaryotic signal transduction (Huang et al. 1996).

In what follows, starting from the mass-action-law kinetics and using a careful perturbation analysis, we derive a consistent approximation of a double-phosphorylation cascade with one variable per cycle (i.e two variables per level). This simplified set of equations enables us to perform a mathematical analysis of the cascade and the construction of the interaction graph for the underlying network. In this way we show that the effect of retroactivity is to provide an intrinsic negative feedback from the variables at each stage of the cascade on the variables of the previous stage. This property is related, as will be explained, to the appearance of sustained oscillations in the cascade.

Previous studies have demonstrated that double phosphorylation of a protein generates bistability if some conditions are fulfilled (Ortega et al. 2006; Markevich et al. 2004), while single phosphorylation cycles have always a single steady-state. In this paper we also show that the bistable behavior originating in a double phosphorylation cycle can reach, due to retroactivity, upper levels of a signaling cascade, unable to display bistability by themselves.

2 A simplified Model for the Double Phosphorylation Cascade

We consider a signaling cascade in which each protein has two phosphorylation sites, as illustrated in Fig. 2. We designate this case as "DP cascade", and distinguish it from the case where only single phosphorylation occurs ("SP cascade"). Cascades involving both single and double phosphorylation cycles are easily described combining the equations for the SP and DP cascades (as it is the case for the MAPK cascade, which involves SP for the first unit and DP for the second and third ones). The three variables in each cycle in Fig. 2, Y_i, Y_i^* and Y_i^{**}, represent the three interconvertible forms of the protein, such as the dephosphorylated, singly and doubly phosphorylated forms; the activated form Y_i^{**} acts as a catalyst for the two activation reactions in the next step. In this cascade, the two deactivation reactions in each step share the same phosphatase, denoted by E_i' First we write the chemical equations. The inter-conversion of the *ith* protein can be described by the following reactions:

$$\begin{aligned}
Y_i + Y_{i-1}^{**} &\underset{d_{i1}}{\overset{a_{i1}}{\rightleftharpoons}} C_{i1} \xrightarrow{k_{i1}} Y_i^* + Y_{i-1}^{**} \\
Y_i^* + Y_{i-1}^{**} &\underset{d_{i2}}{\overset{a_{i2}}{\rightleftharpoons}} C_{i2} \xrightarrow{k_{i2}} Y_i^{**} + Y_{i-1}^{**} \\
Y_i^{**} + E_i' &\underset{d_{i1}'}{\overset{a_{i1}'}{\rightleftharpoons}} C_{i1}' \xrightarrow{k_{i1}'} Y_i^* + E_i', \\
Y_i^* + E_i' &\underset{d_{i2}'}{\overset{a_{i2}'}{\rightleftharpoons}} C_{i2}' \xrightarrow{k_{i2}'} Y_i + E_i', \quad i = 1, \ldots, n,
\end{aligned} \tag{1}$$

where C_{i1}, C_{i2}, C_{i1}' and C_{i2}' are intermediate enzyme-substrate complexes. We take the convention to denote by index 1 and 2 respectively the first and the second

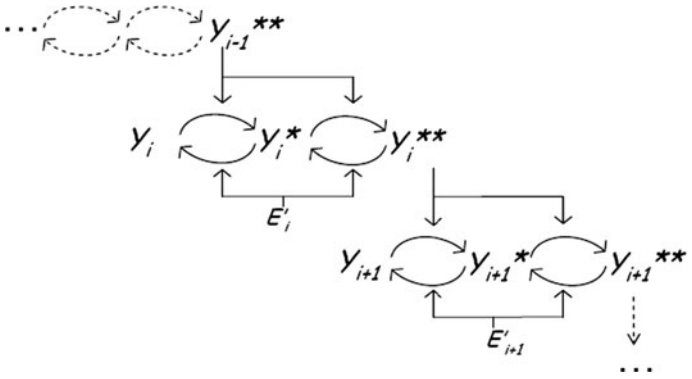

Fig. 2 Schematic representation of a cascade of covalent modification cycles, involving double phosphorylation. The *ith* cycle is composed by three states of the same protein: the inactive, the singly phosphorylated, and the doubly phosphorylated states, labeled Y_i, Y_i^*, and Y_i^{**}, respectively. In each step, the activation is catalyzed by the activated product of the previous step. The deactivation is mediated by another enzyme, E_i'

covalent modifications, starting either from the deactivated species Y_i or from the activated species Y_i^{**}. The notation prime ($'$) is used for the deactivation steps, involving a phosphatase in the case of the dephosphorylation.

Next, the kinetic equations describing the cascade are written using only the law of mass action. For notational convenience we use variable names to denote both a chemical species and its concentration. For instance, the instantaneous state of each cycle is described by the variables Y_i and Y_i^{**}, denoting respectively the concentrations of the inactivated and of the activated protein i, whose total amount is denoted by Y_{iT}. The kinetic equations are explicitly written in "Appendix 1" where we perform a model reduction by using the quasi-steady state approximation. The kinetic equations can be complemented by the corresponding conservation equations: $Y_{iT} = Y_i + Y_i^* + Y_i^{**} + C_{i1} + C_{i2} + C'_{i1} + C'_{i2} + C_{i+1,1} + C_{i+1,2}$ and $E_i^* = E'_i + C'_{i1} + C'_{i2}$

The model reduction starts by considering dimensionless variables, as for instance:

$$y_i^{**} = \frac{Y_i^{**}}{Y_{iT}}, \quad y_i^* = \frac{Y_i^*}{Y_{iT}}, \quad y_i = \frac{Y_i}{Y_{iT}}, \quad c_{ij} = \frac{C_{ij}}{Y_{i-1,T}}, \quad c'_{ij} = \frac{C'_{ij}}{E'_{iT}}. \tag{2}$$

Two key dimensionless parameters are defined to perform the perturbation analysis:

$$\epsilon_i = \frac{E'_{iT}}{Y_{iT}}, \quad \eta_i = \frac{Y_{i-1,T}}{Y_{iT}}. \tag{3}$$

The analysis shows that the state of each doubly phosphorylated cycle can be described by two variables, $x_i = y_i^{**} + c_{i+1,1} + c_{i+1,2}$. As usual, this assumes that the total concentration of phosphatase in the cycle is much lower than the total concentration of targeted protein, resulting in $\varepsilon_i \ll 1$. The other parameters must satisfy:

$$k_{i1}\eta_i \sim k'_{i2}\epsilon_i, \quad k_{i2}\eta_i \sim k'_{i1}\epsilon_i. \tag{4}$$

Finally it is shown in "Appendix 1" that the dynamics of the variables x_i and y_i are described by the following system of differential equations:

$$\dot{x}_i = V_{i2}x_{i-1}\frac{y_i^*}{K_{eff,i2}+y_i^*} - V'_{i1}\frac{x_i}{K'_{eff,i1}+x_i}, \tag{5}$$

$$\dot{y}_i = V'_{i2}\frac{y_i^*}{K'_{eff,i2}+y_i^*} - V_{i1}x_{i-1}\frac{y_i}{K_{eff,i1}+y_i}, \tag{6}$$

with the following conservation equation from which y_i^* has to be extracted:

$$x_i + y_i + y_i^* + \eta_i x_{i-1}\left(\frac{y_i/K_{i1} + y_i^*/K_{i2}}{1 + y_i/K_{i1} + y_i^*/K_{i2}}\right) + O(\epsilon_i) = 1 \tag{7}$$

In the above differential equations, the factors V_i's are defined by:

$$V_{i1} = \frac{k_{i1}\eta_i}{\epsilon}, \quad V_{i2} = \frac{k_{i2}\eta_i}{\epsilon}, \quad V'_{i1} = \frac{k'_{i1}\epsilon_i}{\epsilon}, \quad V'_{i2} = \frac{k'_{i2}\epsilon_i}{\epsilon},$$

where ε is a real number enabling to take the limit where all ε_i and η_i go to 0 at once. (For example, define $\varepsilon_i = a_i\varepsilon$ and $\eta_i = b_i\varepsilon$, with fixed parameters a_i and b_i.) In Eqs. (5)–(6) the effective Michaelis–Menten coefficients $K_{eff,i}$'s are actually functions given by:

$$\begin{aligned}
K_{eff,i1} &= K_{i1}\left(1 + \frac{y_i^*}{K_{i2}}\right),\\
K_{eff,i2} &= K_{i2}\left(1 + \frac{y_i}{K_{i1}}\right),\\
K'_{eff,i1} &= K'_{i1}\left(1 + \frac{y_i^*}{K'_{i2}}\right)\left(1 + \frac{y_{i+1}}{K_{i+1,1}} + \frac{y_{i+1}^*}{K_{i+1,2}}\right),\\
K'_{eff,i2} &= K'_{i2}\left(1 + \frac{x_i}{K'_{i1}\left(1 + \frac{y_{i+1}}{K_{i+1,1}} + \frac{y_{i+1}^*}{K_{i+1,2}}\right)}\right).
\end{aligned} \tag{8}$$

Let us notice that the set of equations Eqs. (5)–(8) in which the effective $K_{eff,i}$'s are replaced by the usual Michaelis–Menten constants K_i's, represent a possible, simple but not rigorous, generalization of the Goldbeter–Koshland model (Goldbeter et al. 1981) to a doubly phosphorylated cascade. This set of phenomenological equations has been used by several authors in order to study properties of the MAPK pathway (Kholodenko 2000; Angeli et al. 2004; Thalhauser and Komarova 2010). As it will be shown in the next sections, the main difference between this new derivation and the simpler case where the $K_{eff,i}$'s are constants, is the dependency of the dynamics at stage i of the cascade on the variables at stage $i + 1$ of the cascade. Moreover we will prove that this retroactivity plays the role of a negative feedback loop on the variables.

3 Intrinsic Negative Feedback and Sustained Oscillations in Biochemical Networks

The existence of autonomous oscillations in biochemical networks can be discussed in the framework of *interaction graphs* associated with dynamical systems. We present a short summary of the underlying theoretical ideas which have been developed in details by several authors (Thomas and D'Ari 1990; Snoussi and Thomas 1993; Gouzé 1998).

3.1 The Interaction Graph of the Doubly-Phosphorylated Signaling Cascade

The deterministic evolution of a biochemical network is usually described by a set of coupled ordinary differential equations in which variables correspond to the concentrations of species $x_i = (x_1, \ldots, x_m)$ and the rates of change of these concentrations are given by nonlinear function of $\dot{x}_i = F_i(x_1, x_2, \ldots, x_m)$. Then one can associate to the network a so-called interaction graph in the following way. The nodes of the graph are simply defined by the species $(x_1, \ldots, x_m)$ concentrations and are labeled by the corresponding integer indexes $1, \ldots, m$. Then, according to the value of $\sigma_{ij} = sign\left(\frac{\partial F_i}{\partial x_j}(x)\right) \in \{0, +1, -1\}$, the nodes i and j are connected by a signed arrow going from x_j to x_i. If $\sigma_{ij} = 0$ there is no arrow. The construction of this graph is motivated by the fact that the elements of the Jacobian matrix, defined by $J_{ij}(x) = \frac{\partial F_i}{\partial x_j}(x)$, describe the instantaneous influence of the node j on the node i of the graph; for example if $J_{ij}(x) > 0$ it means that the rate of change of x_j increases if a positive perturbation of x_j occurs, and conversely decreases if the perturbation of x_j is negative. Therefore when an edge of the graph is positive $\sigma_{ij} > 0$ one can say that node j "activates" or "excites" node i of the graph. Conversely, a negative edge in the graph, $\sigma_{ij} < 0$, means that node j "inhibits" or "represses" node i of the network. In particular $\sigma_{ij} = 0$ tells ones that the nodes i and j are uncoupled. In several instances of biological networks (e.g. neural networks, genetic networks, ecological networks), although the value of $J_{ij}(x)$ depends on x, its sign is constant in all the phase space (Thomas and D'Ari 1990). In this case it is meaningful to qualitatively characterize the biochemical network by its interaction graph. Moreover, several qualitative properties about the dynamics of a biochemical network can be deduced from the knowledge of its interaction graph (Thomas and D'Ari 1990). These properties rely on the concept of circuit in the graph, that is an oriented and closed path linking a series of connected nodes in the interaction graph. The notion of semi-circuit is defined as the concept of circuit but on the non-oriented graph. The sign of a circuit or of a semi-circuit in the interaction graph is defined by the product of the signs of the edges along the path defining the circuit.

Amongst those properties, we recall a conjecture of Thomas proved by Gouzé in (1998) : A necessary condition to get sustained periodic oscillations in a differential system $\dot{x}_i = f_i(x_1, \ldots, x_m)$ is the existence of a negative semi-circuit of length at least 2 in its interaction graph.

Let us apply this result to biochemical networks which are the double-phosphorylation signaling cascades. Figures 3 show two possible interaction graphs for such systems. The first one, Fig. 3a, depicts the interaction graph deduced from a simplified model used in the literature for describing DP cascades (Kholodenko 2000; Angeli et al. 2004), that is the set of Eqs.(5)–(6) where the Michaelian parameters $K_{eff,i}$ are constant. Indeed this first type of interaction graph seems to be consistent with the usual picture of one-way signaling cascade drawn in Fig. 2. In this case one sees that there are no negative feedback loops. At each level of the cascade there are 2 arrows going from one stage to the next stage, with a positive interaction from x_i to x_{i+1} and a negative interaction from x_i to y_{i+1}. Inside one stage there are 2 negative interactions so that any circuit in the whole interaction graph is a positive circuit. Therefore, according to the Thomas' rule proved by Gouzé, autonomous oscillations should never be observed in double phosphorylation cascades following this interaction graph. Moreover, in order to produce oscillations in this system, it would be necessary to consider extra negative interactions, like for example a negative interaction between the doubly phosphorylated protein in the last stage of the cascade and the activation at the first stage of this system. Such setting has been proposed and oscillations theoretically studied in this framework (Kholodenko 2000).

On the other hand, in Qiao et al. (2007) the authors numerically explored the possible behaviors of the MAPK cascades, without extra feedbacks, by considering an extensive sampling of the parameter space around experimental values studied by Huang et al. (1996). Amongst the results of their investigations they observed the occurrence of autonomous oscillations in about 9 % of their sampled parameters. Although they did not discuss the relation between their findings and the interaction graphs, according to the theorem recalled above, the interaction graph of the MAPK cascade should contain inherent negative feedback loops.

Therefore we study the DP signaling cascade by looking for negative feedback loops in its interaction graph. As we already pointed out, our new 1-variable per cycle model described by Eqs.(5)–(7) shows the existence of a coupling of one of the variables at one stage of the cascades with the variables of the preceding stage. In order to construct the interaction graph of this system, we have computed the matrix elements of the Jacobian matrix corresponding to the interaction of variables at stage $i+1$ on variables at stage i. The resulting computation, reported in "Appendix 2", shows that the variables at stage $i+1$ have all negative influences on the variables at stage i:

$$\frac{\partial \dot{x}_i}{\partial x_{i+1}} < 0 \quad \frac{\partial \dot{x}_i}{\partial y_{i+1}} < 0 \quad \frac{\partial \dot{y}_i}{\partial x_{i+1}} < 0 \quad \frac{\partial \dot{y}_i}{\partial y_{i+1}} < 0 \tag{9}$$

Figure 3b illustrates the corresponding interaction graph of the DP signaling cascades as it can be computed from our simplified model.

Therefore, the negative retroactivity between the variables of one stage of the cascade with the previous stage creates several negative closed circuits between the cascade stages. For example there is a negative feedback loop between variables x_i and x_{i+1}. So our study reconciliates the fact that sustained oscillations exist in the DP signaling cascade with a consistent description of its interaction graph.

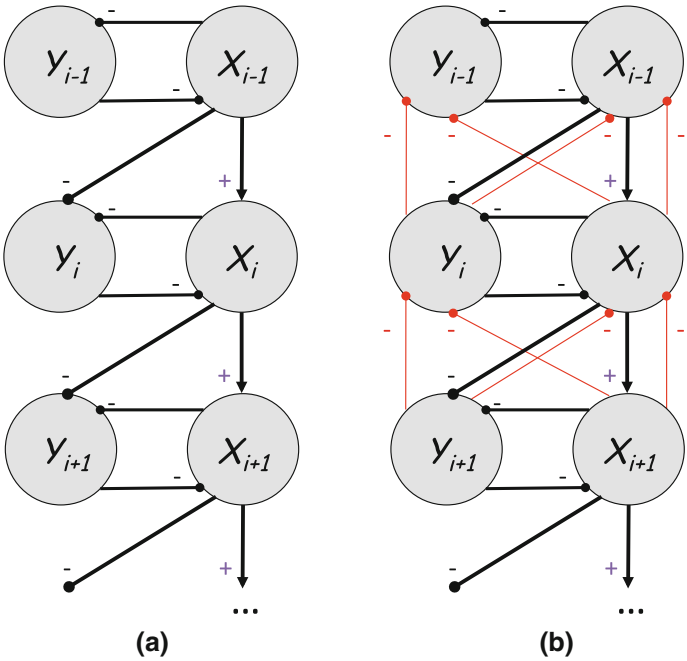

Fig. 3 Interaction graph of the doubly-phosphorylated cascade. **a** According to the phenomenological model (see text). **b** According to Eqs.(5)–(7) that we derived in order to take into account retroactivity from one stage of the cascade on the previous one

3.2 The Simplest Cascade Admitting a Sustained Oscillatory Dynamics

In order to observe how sustained oscillations can show up in a signaling cascade as a consequence of retroactivity, *i.e* the mentioned intrinsic negative feedback, we wish to study the simplest situation where they can occur. A priori the simplest situation would be to consider the single-phosphorylation cascade, because the interaction graph of this system already possesses the negative loops necessary for the existence of oscillations (Ventura et al. 2008). However, as we have already numerically explored this system in a previous work, temporal oscillations can be excited in the single-phosphorylated cascade but these oscillations are strongly damped (Ventura et al. 2008). Indeed, the presence of negative feedback loops in the interaction graph of a biochemical network is a necessary but not sufficient condition to get sustained oscillations in the temporal dynamics of the system. As a matter of fact, the presence of a double phosphorylation seems to be necessary in order to observe autonomous oscillations in a cascade.

Therefore, we consider the simplified signaling chain formed by the top part of the MAPK cascade; thus the first stage of the cascade is made of a single phosphorylation cycle and the second stage is made of double-phosphorylation cycles (cf. Fig. 9). This appears to be the minimal model to study the sought oscillations because, as it is argued below, it enables the second stage of the cascade to exhibit a bistability of steady states. The simplified model of such system is given

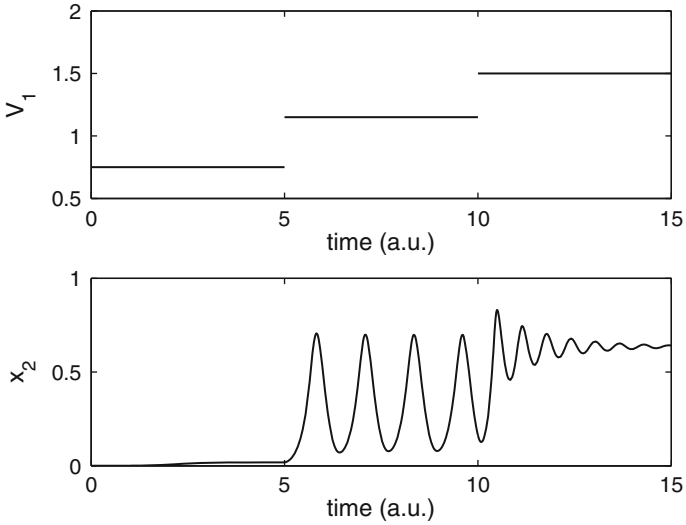

Fig. 4 Time evolution of the doubly phosphorylated protein $y_2^{**} = x_2$ is shown whereas the input parameter V_1 of the cascade is varied in 3 steps. The two-stage signaling cascade is modelled by Eqs.(10)–(12), the first stage being a single-phosphorylation and the second stage being a double-phosphorylation. The bifurcation parameter V_1 is proportional to the total kinase of the first stage (E_{1T}). The parameter values are $0 < V_1 < 2, V_1' = 4, V_{22} = 1.210^2, V_{21} = V_{21}' = V_{22}' = 10^2, K_1 = K_1' = 10^{-1}$, $K_{12} = K_{22} = K_{21}' = K_{22}' = 10^{-2}$

by a set of 3 coupled differential equations, which are a particular case of system of Eqs. (5)–(7), and which can be written as follows:

$$\dot{x}_1 = V_1 \frac{y_1}{K_1 + y_1} - V_1' \frac{x_1}{K_1'(1 + y_2/K_{21} + y_2^*/K_{22}) + x_1} \tag{10}$$

$$\dot{x}_2 = V_{22} x_1 \frac{y_2^*}{K_{22}(1 + y_2/K_{21}) + y_2} - V_{21}' \frac{x_2}{K_{21}'(1 + y_2^*/K_{22}') + x_2} \tag{11}$$

$$\dot{y}_2 = V_{22}' \frac{y_2^*}{K_{22}'(1 + x_2/K_{21}') + y_2^*} - V_{21} x_1 \frac{y_2}{K_{21}(1 + y_2^*/K_{22}) + y_2} \tag{12}$$

with the approximate conservation law : $y_1 = 1 - x_1$, $y_2^* = 1 - x_2 - y_2$

We numerically study the "response" of the system as the evolution of variable $y_2^{**} = x_2$ following the changes of the input parameter V_1. The latter is the natural control parameter, since it is proportional to the total kinase concentration in the first stage of the cascade (E_{1T}). Figure 4 shows an instance of output of the system when V_1 takes 3 different values. When the input enzyme is sufficiently low or high, the response of the system is as usual stationary and corresponds respectively to an inactivated or to an activated state of the doubly phosphorylated protein in the second stage of the cascade. By contrast, for intermediate values of the input kinase, the response of the system varies periodically in time between its activated and deactivated states. For the upper value of V_1, oscillations exist but are damped.

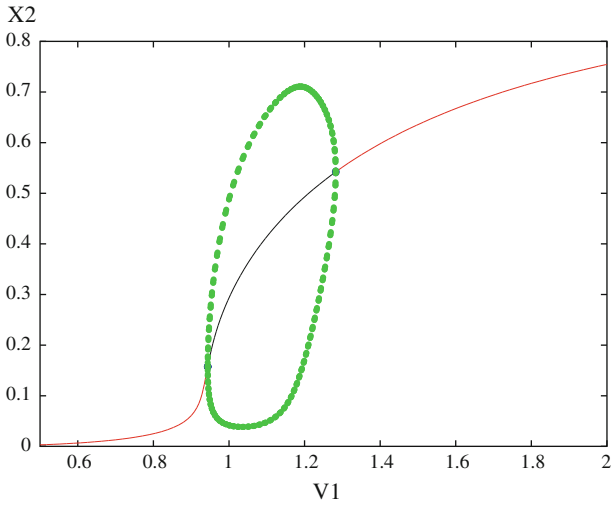

Fig. 5 The continous curve shows the steady state response of variable x_2 in function of V_1 (i.e. the maximal velocity of the upstream enzymatic reaction, proportional to the input enzyme E_{1T}. The steady state is unstable in the intermediate region limited by the *small circles* on the curve. The latter corresponds to Hopf bifurcation points, leading to a limit cycle in the intermediated region of parameters. There, the *dotted curve* shows the extrema of the oscillation amplitudes of x_2. The parameter values are the same as in Fig. 4

These time-dependent behaviors of the cascade variables indicate that the steady state response becomes unstable in a range of V_1 parameter. To investigate the nature of this instability we used XPPAUT software (http://www.math.pitt.edu/bard/xpp/xpp.html) to perform a numerical continuation of the steady state in function of parameter V_1. As shown on Fig. 5 (continuous curve), the steady state values of the doubly phosphorylated proteins in the cascade follows a typical ultrasensitive response in function of the input enzyme. However, the intermediate values (inside the dotted closed curve drawn on the graph) correspond to an unstable output, that would not be observed in an usual dose/response experiment. Instead, self-sustained oscillations would occur, whose maxima and minima amplitudes are also plotted on Fig. 5 The continuation method XPPAUT reveals that the oscillations appear and disappear through supercritical Hopf bifurcations. In particular, the amplitude starts from 0 and the period of oscillations is finite at the bifurcation points.

In order to understand the mechanisms behind the onset of oscillations, it is instructive to look at the phase portrait of this system. From a general point of view, the 3-dimensional phase space subtended by the system variables (x_1, y_2, x_2) could be relatively complicated. However one can look for simplifying hypothesis in order to consider only the subspace subtended by variables (x_1, x_2). For example, in the particular case where $K_{21} = K_{22}$, one notices that the surface defined by $\dot{x}_1 = 0$ has a graph which is independent on y_2. Therefore its projection on the subspace (x_1, x_2) defines a curve, which plays the role of a nullcline. The latter is represented by the dashed (blue) line on Fig. 6. On the same subspace (x_1, x_2), one can represent the curve defined by $\dot{x}_2 = 0 \, and \, \dot{y}_2 = 0$, drawn as a dash-dot (red) curve on Fig. 6.

Then, the intersection of this curve with the surface $\dot{x}_1 = 0$ corresponds to a steady state of the dynamical system.

Moreover, it turns out that the nullcline defined by the equations ($\dot{x}_2 = 0$ *and* $\dot{y}_2 = 0$) is s-shaped. This can be interpreted by noting that the double-phosphorylation cycle possesses a domain of bistable steady states as a function of its input kinase x_1. Furthermore, as a matter of fact, the flow along this s-shaped nullcline points towards the folds of the bistable curve (cf. arrows on Fig. 6). Therefore, these qualitative conditions favour the creation of a flow rotating around the steady state in phase space, leading possibly to a limit cycle. This scenario is confirmed by using a numerical method that reveals Hopf bifurcations, as described above. In the meantime we understand that the oscillations persist only in a range of parameter V_1. Indeed, a change of this parameter affects the position of the surface $\dot{x}_1 = 0$ (dashed line on Fig. 6), in such a way that for low or high values of the parameter V_1, the steady state moves respectively on the lower or on the upper branch of the s-shaped curve, leading to the disappearance of oscillations.

4 Bistability

4.1 Bistability in an Isolated Double-Phosphorylation Cycle

We first consider an isolated double-phosphorylation cycle as shown in Fig. 7. As illustrated, the interconvertible protein exists in three forms: unmodified (Y_i), with one modified residue (Y_i^*) and with two modified residues (Y_i^{**}). As before, we consider the standard two-step reaction model for enzymatic reactions. Let E_i be the converter enzyme that converts Y_i into (Y_i^*) and (Y_i^*) into (Y_i^{**}), and let E_i' be the converter enzyme that converts back (Y_i^{**}) into (Y_i^*) and (Y_i^*) into Y_i. The reactions for the system are as in Eqs. (1) but replacing Y_{i-1}^{**} by E_i.

In this section and since we want to solve for the steady-states of the system, we could either use the simplified kinetic equations for the cascade as in Sect. 3.2 or the full mechanistic model because both models share the same steady-states (provided that in both cases we use a simplified conservation law, see below). The steady-states are obtained by solving:

$$\begin{aligned} v_1 &= v_2' \\ v_1' &= v_2 \end{aligned} \tag{13}$$

with

$$\begin{aligned} v_1 &= \frac{V_{m1} y_i / K_1}{1 + y_i/K_1 + y_i^*/K_2} \qquad v_2 = \frac{V_{m2} y_i^*/K_2}{1 + y_i/K_1 + y_i^*/K_2} \\ v_1' &= \frac{V'_{m1} y_i^{**}/K_1'}{1 + y_i^{**}/K_1' + y_i^*/K_2'} \qquad v_2' = \frac{V'_{m2} y_i^*/K_2'}{1 + y_i^{**}/K_1' + y_i^*/K_2'} \end{aligned} \tag{14}$$

Some definitions used above: $y_i = Y_i/Y_T, y_i^* = Y_i^*/Y_T$ and $y_i^{**} = Y_i^{**}/Y_T$ are the dimensionless concentrations of species Y_i, (Y_i^*) and (Y_i^{**}), and Y_T is the total

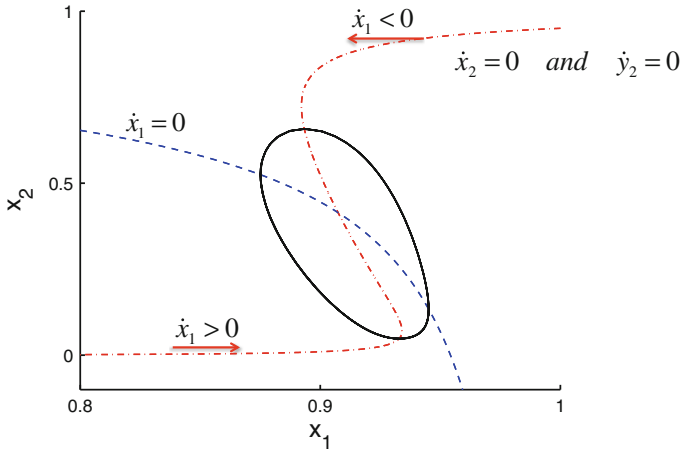

Fig. 6 Autonomous oscillations appearing in a two-stage signaling cascade modelled by Eqs.(10)–(12), with same parameters as in Fig. 4. Plotting the nullclines in the subspace (x_1,x_2) reveals the unstable steady state around which exists a limit cycle (*closed curve*). See text for further discussion. (Color figure online)

concentration of the interconvertible protein Y; $K_i = K_{mi}/Y_T$, where K_{mi} is the Michaelis constant, $V_{mi} = k_i E_T$ and $V'_{mi} = k'_i E'_T$ for i = 1, 2 are the maximal rates of step i. For convenience and following the calculations in (Ortega et al. 2006), we define the following parameters: $r = V_{m2}/V_{m1}$, $r' = V'_{m2}/V'_{m1}$, $\chi = V_{m1}/V'_{m1}$ and $\theta = rr'$.

Assuming $K_1 = K'_1 = K_2 = K'_2 \equiv K$ for the sake of simplicity, the following is obtained manipulating Eqs. (14):

$$\theta = \frac{y_i y_i^{**}}{y_i^{*2}} \tag{15}$$

Assuming a simplified conservation equation, $1 = y_i + y_i^* + y_i^{**}$, leads to:

$$\begin{aligned} y_i &= \frac{\left(-y_i^{**} + \sqrt{y_i^{**2} + 4y_i^{**}\theta - 4y_i^{**2}\theta}\right)^2}{4y_i^{**}\theta} \\ y_i^* &= \frac{-y_i^{**} + \sqrt{y_i^{**2} + 4y_i^{**}\theta - 4y_i^{**2}\theta}}{2\theta} \\ \chi &= \frac{y_i^{**}K + y_i^{**}y_i^* + \theta y_i^{*2}}{r_{21}y_i^*(K + y_i^{**} + y_i^*)} \end{aligned} \tag{16}$$

The equations above are providing y_i and Y_i^*as a function of Y_i^{**} and parameters, and also and implicit equation for Y_i^* [the algebraic manipulations required the obtain these equations were guided by Ortega et al. (2006)]. This last equation permits to calculate the bifurcation point, for further details see Ortega et al. (2006). Figure 8 shows that, for the selected parameter values, there is a range of χ that provides bistable behavior for the double-phosphorylation cycle.

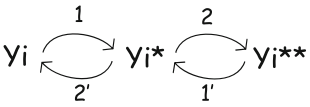

Fig. 7 Isolated double-phosphorylation cycle. Steps 1 and 2 are those that add the first and second covalent modification, respectively, while steps 1′ and 2′ those that remove them

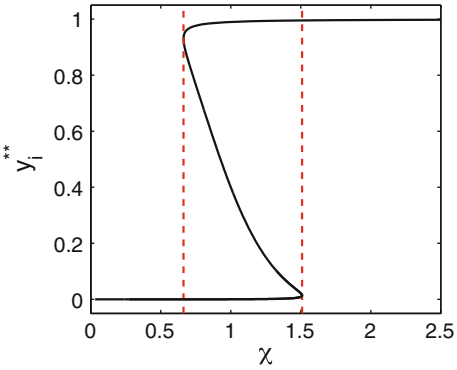

Fig. 8 Variation of Y_i^{**} with respect to χ. Parameter values are: $\theta = 4$, $r = 2$, $K = 0.01$. *Red dashed lines* indicates the range of χ that leads to two stable solutions for Y_i^{**}. (Color figure online)

From the calculations above we can also derive the amount of free kinase E_i as follows:

$$E_i = \frac{E_{iT}}{1 + y_i/K_1 + y_i^*/K_2} \tag{17}$$

Given that y_i and Y_i^* display bistability for a given range of parameters, the same is true for the free amount of kinase E_i. This result still holds if the double-phosphorylation cycle is coupled to an upstream cycle that activates E_i, as we will show in the following section.

4.2 Double-Phosphorylation Cycle's Effect on an Upstream Cycle

We now consider a 2-stage cascade composed of a singly-phosphorylated protein activating a double-phosphorylation cycle, as indicated in the scheme in Fig. 9. Protein Y_1 is transformed into (Y_i^*) by the action of an activator enzyme A and (Y_i^*) back into Y_1 by the action of an inactivator enzyme D.

In "Appendix 3" we include a detailed calculation of the steady-states for this cascade that leads to the following results:

$$y_1^* = \frac{1}{(1+\omega) + y_2/K + y_2^*/K} \tag{18}$$

$$\chi = \frac{y_2^{**}K(1+\omega) + y_2^{**}y_2^* + \theta y_2^{*2}}{r y_2^*(K + y_2^{**} + y_2^*)} \tag{19}$$

with y_2 and y_2^* exactly as in Eq. (16). We are still considering equal K values for all the reactions in the second stage just for the sake of simplicity and we are

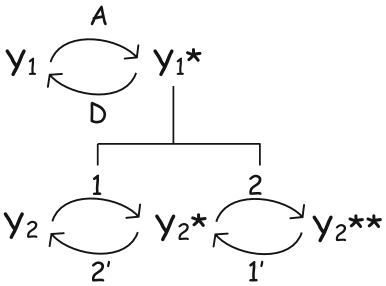

Fig. 9 2-stages cascade composed by a single-phosphorylation cycle and a double-phosphorylation one

simplifying notation in χ and r. Parameter ω is defined as $(k' K_m D)/(k K_m' A)$, where k and k' are the catalytic rates and K_m and K_m' are the Michaelis constants for the upper cycle, and A and D are the amounts of activator and inactivator assumed to be approximately constant (see "Appendix 3"). So ω contains the information on the upper cycle and is reduced to zero if there is no inactivator, as in the previous section. ω appears in the equation relating χ and y_i^{**} in such a way that it does not change the properties of this implicit equation for y_i^{**}, i.e., there is still a range of parameters for which bistability is observed, see Fig. 10a.

Interestingly and according to Eq. (18), y_1^* depends on y_2 and y_2^*, which depend on y_2^{**} [see Eq. (16)], which has a bistable behavior, meaning that y_1^* is itself bistable as well, as illustrated in Fig. 10b.

5 Discussion and Conclusion

In recent years the study of signaling pathways, and in particular of MAPK signaling cascades, has retained much attention in systems biology because it is currently believed that acquiring a deep understanding of this type of system could help to design new therapies against several pathological conditions such as cancer (Ventura et al. 2009, Wagner and Nebreda 2009). Remarkably, in biochemistry articles or textbooks, the signaling cascades are graphically represented by a series of reactants (possibly detailing their activation by rapid interconverting species) that are connected only by feedforward arrows. Each step in the chain is an enzymatic reaction that is catalyzed by the activated reactant at the previous stage. However, as we had already pointed out in a previous work, the usual graphical representation of cascades in terms of enzymatic chemical reactions can elude the possible retroactivity phenomenon appearing in these systems, due to the temporary sequestration of the enzymes by their target reactants.[1] In (Ventura et al. 2008) this retroactivity phenomenon was analyzed in the simplest case, namely when a single covalent modification occurs at each step of the cascade. In the present paper we have analyzed the more complex case of double covalent modifications at each

[1] Generally speaking, it would be desirable, in graphical representations of biochemical reactions, to use a specific type of arrow-symbol, whenever the phenomenon of sequestration is involved.

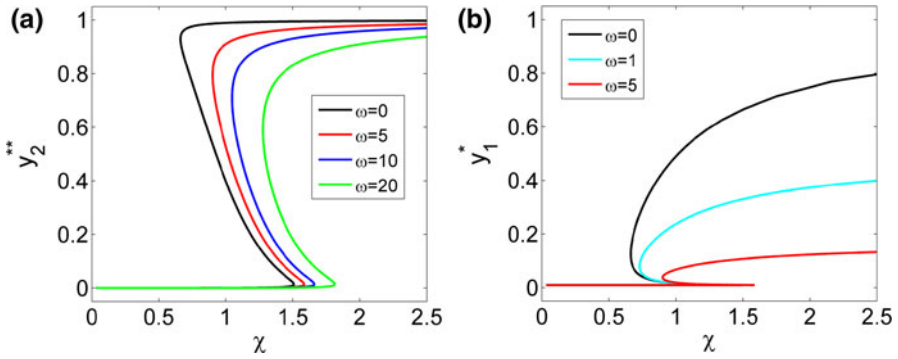

Fig. 10 **a** Variation of y_2^{**} in a 2-stage cascade, with respect to parameter χ. Parameter values are: $\theta = 4$, $r = 2$, $K = 0.01$, and different values of ω as indicated. **b** Variation of y_1^{**} in a 2-stage cascade, with respect to parameter χ. Parameter values as in **a**, ω values as indicated

stage of the cascade. This work was indeed motivated by the study of the MAPK signaling cascades, that are characterized by stages where a double phosphorylation are necessary to activate the reactant kinase.

Following the same theoretical method as used in (Ventura et al. 2008), we have derived a simplified model of the kinetic equations of the cascade, with only one variable characterizing each phosphorylation/dephosphorylation cycle. The interest of the analysis was not only to achieve a simplified model of the cascade dynamics, but overall to show a form of the kinetic equations where the retroactivity phenomenon clearly appears in the functional dependency of the variables. Indeed the resulting equations have the typical Michaelian form but with effective Michaelis–Menten factors which are in fact functions depending on the variables associated with the next stage in the cascade. This simplification enables one to explicitly compute the corresponding Jacobian matrix elements and to prove that the retroactive interaction is always a negative feedback. Interestingly, the existence of a negative feedback in the structure of the MAPK cascade had been demonstrated in Fages and Soliman (2008), by using a computarized algorithmic method. The interpretation of this result was made clearer by our analytical study which indicates that the origin of this negative feedback is a sequestration effect.

The interaction graph of the double phosphorylation cascade was computed and showed on Fig. 3. By examining that structure it is seen that several positive and negative feedback loops can be drawn. Therefore the so-called Thomas rules (Thomas and D'Ari 1990) are met, opening the possibility to observe autonomous oscillations, as well as multistable behaviors in the dynamics. In fact, sustained oscillations and bistability in a cascade, with at least one level having double-phosphorylation, were reported in previous works. First of all, building on the pioneering work of Huang et al. (1996), Qiao et al. (2007) conducted a systematic numerical study of a detailed modeling of the MAPK cascade, where they discovered a significative region of the parameter space where sustained oscillations occured. In particular, by restricting the modeling to the different components of the signaling cascade, they found that the minimal network to get autonomous

oscillations was a single-phosphorylation cycle connected to a double phosphorylation cycle. This scheme corresponds, for instance, to the top part of the MAPK cascade (Raf–Mek–Erk). These results were further studied by Zumsande and Gross (2010), who applied their approach of generalized modeling to the study of complex dynamical behaviors of MAPK cascades. The idea of this approach is to identify the bifurcations of the system within a whole class of plausible models, by parametrizing the underlying Jacobian matrix of the system equations, rather than parametrizing the rate laws in the model (Gross and Feudel 2006). Using this method, these authors found that a cascade made of a single phosphorylation cycle activating a double phosphorylation layer could exhibit Hopf bifurcations and thereby lead to the existence of autonomous oscillations. Let us note that the generalized modeling method indicated that more complex dynamics and chaos could arise in the MAPK cascade with at least 3 layers, due to the existence of double Hopf bifurcation (Zumsande and Gross 2010). Corroborating these previous studies, our work points out the essential role of the retroactivity in the onset of sustained oscillations in MAPK signaling cascades. Indeed, we showed that here the retroactivity gives rise to intrinsic negative circuits in the interaction graph of these systems, a property that is necessary for the existence of autonomous oscillations. Moreover we demonstrated that this feature is preserved in a class of simplified kinetic equations of signaling cascades, that we rigorously derived from a scheme based on the quasi-steady state approximations.

Using the simplified dynamics describing the top part of the MAPK cascade we recover that indeed it is the minimal model to get autonomous oscillations in a signaling cascade. These oscillations appear and disappear through Hopf bifurcations, when the input kinase in the first cycle has intermediate values between the ones leading to the inactivation or the activation of the cascade.

It is well known that covalent modification cycles with single phosphorylation only allow a single steady-state (Feliu and Wiuf 2012), whereas double-phosphorylation allows a bistability of steady states, for appropriate parameters (Ortega et al. 2006). In the last section of this paper, our results show that when a cascade is formed by two such systems, the bistability of the DP cycle can persist, and moreover is transmitted to the state variable of the first layer formed by the SP cycle. Therefore the SP cycle can acquire a bistable behavior due to its interaction on the second layer.

In conclusion, our studies showed the existence of interesting phenomena—oscillations and transmitted bistability—in signaling cascades possessing at least one stage with a DP cycle. In order to account for these phenomena it is crucial to consider the intrinsic feedback, or the retroactivity, existing between one stage and the previous stage in these signaling cascades. From the theoretical side, this retroaction is clearly set in evidence by our simplified set of equations, obtained in the framework of a rigorous quasi-steady state approximation.

Acknowledgments The international program of scientific collaboration PICS 05922 between CNRS (France) and CONICET (Argentina) is acknowledged. ACV is a member of the Carrera del Investigador Cientfico (CONICET) and was supported by the Agencia Nacional de Promoción Cient fica y Tecnolgica (Argentina).

Appendix 1: Simplified Kinetic Equations of the Double phosphorylation cascade

In this appendix we show how the 1-variable per cycle model (5)–(8) can be obtained from a singular perturbation analysis of the full mass-action kinetic equations. The procedure is standard, e.g. (Murray 2002).

According to the scheme in Eqs. (1), and using only the law of mass action, the dynamics of the *ith* cycle in a cascade of n cycles is governed by the conservation equations $Y_{iT} = Y_i + Y_i^* + Y_i^{**} + C_{i1} + C_{i2} + C'_{i1} + C'_{i2} + C_{i+1,1} + C_{i+1,2}$ and $E'_{iT} = E'_i + C'_{i1} + C'_{i2}$ and by the following differential equations:

$$\begin{aligned}
\frac{dY_i^{**}}{dt} &= k_{i2}C_{i2} - a'_{i1}Y_i^{**}E'_i + d'_{i1}C'_{i1} - a_{i+1,1}Y_{i+1}Y_i^{**} + (k_{i+1,1} + d_{i+1,1})C_{i+1,1} \\
&\quad - a_{i+1,2}Y_{i+1}^{*}Y_i^{**} + (k_{i+1,2} + d_{i+1,2})C_{i+1,2} \\
\frac{dY_i}{dt} &= k'_{i2}C'_{i2} - a_{i1}Y_iY_{i-1}^{**} + d_{i1}C_{i1} \\
\frac{dC_{i1}}{dt} &= a_{i1}Y_iY_{i-1}^{**} - (k_{i1} + d_{i1})C_{i1} \\
\frac{dC_{i2}}{dt} &= a_{i2}Y_i^{*}Y_{i-1}^{**} - (k_{i2} + d_{i2})C_{i2} \\
\frac{dC'_{i1}}{dt} &= a'_{i1}Y_i^{**}E'_i - (k'_{i1} + d'_{i1})C'_{i1} \\
\frac{dC'_{i2}}{dt} &= a'_{i2}Y_i^{*}E'_i - (k'_{i2} + d'_{i2})C'_{i2}
\end{aligned} \tag{20}$$

with $i = 1, \ldots n$, with the convention that Y_0^{**} is related to the input stimulus, whereas $Y_{n+1} = C_{n+1,\,j} = 0$ $(j = 1,2)$.

As described in Sect. 2, we define the parameters $\varepsilon_i = E'_{iT}/\ Y_{iT}$ and $\eta_i = Y_{i\text{-}1,T}/\ Y_{iT}$. Michaelis constants are defined as usual as $K_{ij} = (k_{ij} + d_{ij})/a_{ij}$ and $K'_{ij} = (k'_{ij} + d'_{ij})/a'_{ij}$. We define also new variables $X_i = Y_i^{**} + C_{i+1,1} + C_{i+1,2}$ that reveal to be natural slow variables of the system. The variables are turned into dimensionless ones in the following way:

$$x_i = \frac{X_i}{Y_{iT}}, \quad y_i = \frac{Y_i}{Y_{iT}}, \quad c_{ij} = \frac{C_{ij}}{Y_{i-1,T}}, \quad c'_{ij} = \frac{C'_{ij}}{E'_{iT}}, \quad e'_i = \frac{E'_i}{E'_{iT}}. \tag{21}$$

The previous system of ODEs can be then written as:

$$\frac{dx_i}{dt} = \eta_i k_{i2}c_{i2} - \epsilon_i k'_{i1}c'_{i1} - \epsilon_i a'_{i1}Y_{iT}\left[(x_i - c_{i+1,1} - c_{i+1,2})e'_i - K'_{i1}c'_{i1}\right] \tag{22}$$

$$\frac{dy_i}{dt} = \epsilon_i k'_{i2}c'_{i2} - \eta_i k_{i1}c_{i1} - \eta_i a_{i1}Y_{iT}\left[y_i(x_i - c_{i+1,1} - c_{i+1,2}) - K_{i1}c_{i1}\right] \tag{23}$$

$$\frac{dc_{i1}}{dt} = a_{i1}Y_{iT}(y_i(x_{i-1} - c_{i1} - c_{i1}) - K_{i1}c_{i1}) \tag{24}$$

$$\frac{dc_{i2}}{dt} = a_{i2}Y_{iT}\left(y_i^*(x_{i-1} - c_{i1} - c_{i1}) - K_{i2}c_{i2}\right) \tag{25}$$

$$\frac{dc'_{i1}}{dt} = a'_{i1} Y_{iT}\left((x_i - c_{i+1,1} - c_{i+1,2})e'_i - K'_{i1}c'_{i1}\right) \tag{26}$$

$$\frac{dc'_{i2}}{dt} = a'_{i2} Y_{iT}\left(y^*_i e'_i - K'_{i2}c'_{i2}\right) \tag{27}$$

with $i = 1, \ldots, n$, with again the convention that in these equations $c_{n+1,j} = 0$, and $x_0 = S$ denotes the input stimulus (e.g. some available active enzyme) normalized by $\eta_1\, Y_{1T}$. Here the conservation laws become $x_i + y^*_i + y_i + \eta_i(c_{i1} + c_{i2}) + \epsilon_i(c'_{i1} + c'_{i2}) = 1$ and $c'_{i1} + c'_{i2} + e'_i = 1$.

Now, in the limit where all $\epsilon_i \to 0$, and assuming that $k_{i1}\eta_i \sim k'_{i2}\epsilon_i$ and $k_{i2}\eta_i \sim k'_{i1}\epsilon_i$, we get a slow dynamics for the variables x_i and y_i as compared with the rates of change of the complexes c_i and c'_i, so that the quasi-steady state approximation can be applied. Let us assume that ϵ is a representative value of the set $\{\epsilon_1, \epsilon_2, \cdots, \epsilon_n\}$ and consider a slow time-scale $\tilde{t} = \epsilon t$ with the time-derivative with respect to $\tilde{t}$ that is denoted by a dot, i.e. $\dot{x} = dx/d\tilde{t}$. By imposing that $\dot{c}_{ij} = \dot{c}'_{ij} = 0$, a little calculation gives:

$$\begin{aligned}
c_{i1} &= x_{i-1}\frac{y_i/K_{i1}}{1 + y_i/K_{i1} + y^*_i/K_{i2}}\\
c_{i2} &= x_{i-1}\frac{y^*_i/K_{i2}}{1 + y_i/K_{i1} + y^*_i/K_{i2}}\\
c'_{i1} &= \frac{x_i/K'_{i1}}{(1 + y_{i+1}/K_{i+1,1} + y^*_{i+1}/K_{i+1,2})(1 + y^*_i/K'_{i2}) + x_i/K'_{i1}}\\
c'_{i2} &= \frac{y^*_i/K'_{i2}}{1 + y_i/K'_{i1} + y^*_i/K'_{i2}}
\end{aligned}$$

Finally, the substitution of these expressions in Eqs. (22) gives the new model Eqs. (5)–(8), with $V_{ij} = k_{ij}\eta_i/\epsilon$ and $V'_{ij} = k'_{ij}\epsilon_i/\epsilon$.

Appendix 2: Computation of the Interaction Graph

In this Appendix we prove inequalities (9) in order to show that in the interaction graph (Fig. 3) the variables at stage $i + 1$ of the cascade have a negative influence on the variables at stage i. This can be achieved by computing the corresponding elements of the Jacobian matrix as follows :

$$\frac{\partial \dot{x}_i}{\partial x_{i+1}} = \frac{V'_{i1}x_i}{(K'_{eff,i1} + x_i)^2}\frac{K'_{i1}\left(1 + \frac{y^*_i}{K'_{i2}}\right)}{K_{i+1,2}}\frac{\partial y^*_{i+1}}{\partial x_{i+1}} \tag{28}$$

$$\frac{\partial \dot{x}_i}{\partial y_{i+1}} = \frac{V'_{i1}x_i}{(K'_{eff,i1} + x_i)^2}\frac{K'_{i1}\left(1 + \frac{y^*_i}{K'_{i2}}\right)}{K_{i+1,2}}\frac{\partial y^*_{i+1}}{\partial y_{i+1}} \tag{29}$$

$$\frac{\partial \dot{y}_i}{\partial x_{i+1}} = \frac{V'_{i2}y^*_i}{(K'_{eff,i2} + y^*_i)^2}\frac{K'_{i2}x_i}{K'_{i1}\left(\frac{y_{i+1}}{K_{i+1,1}} + \frac{y^*_{i+1}}{K_{i+1,2}}\right)^2 K_{i+1,2}}\frac{\partial y^*_{i+1}}{\partial x_{i+1}} \tag{30}$$

$$\frac{\partial \dot{y}_i}{\partial y_{i+1}} = \frac{V'_{i2} y_i^*}{\left(K'_{eff,i2} + y_i^*\right)^2} \frac{K'_{i2} x_i}{K'_{i1}\left(\frac{y_{i+1}}{K_{i+1,1}} + \frac{y_{i+1}^*}{K_{i+1,2}}\right)^2 K_{i+1,2}} \frac{\partial y_{i+1}^*}{\partial y_{i+1}} \tag{31}$$

and the remaining partial derivatives can be computed by using the conservation law (7). These factors are always negative:

$$\frac{\partial y_{i+1}^*}{\partial x_{i+1}} = -\left(\frac{1}{1 + \eta_{i+1} x_i \frac{1/K_{i+1,2}}{\left(1 + y_{i+1}/K_{i+1,1} + y_{i+1}^*/K_{i+1,2}\right)^2}}\right)$$

$$\frac{\partial y_{i+1}^*}{\partial y_{i+1}} = -\left(\frac{1 + \eta_{i+1} x_i \frac{1/K_{i+1,1}}{\left(1 + y_{i+1}/K_{i+1,1} + y_{i+1}^*/K_{i+1,2}\right)^2}}{1 + \eta_{i+1} x_i \frac{1/K_{i+1,2}}{\left(1 + y_{i+1}/K_{i+1,1} + y_{i+1}^*/K_{i+1,2}\right)^2}}\right)$$

Appendix 3: Computation of the Steady-States for a 2-Stage Cascade

We consider the following reactions for the upper cycle in Fig. 9:

$$\begin{aligned} Y_1 + A &\underset{d}{\overset{a}{\rightleftharpoons}} C_A \xrightarrow{k} Y_1^* + A \\ Y_1^* + D &\underset{d'}{\overset{a'}{\rightleftharpoons}} C_D \xrightarrow{k'} Y_1 + D \end{aligned} \tag{32}$$

with A and D the activator and inactivator enzymes, respectively. Assuming A and D are approximately constants and solving for the steady-states, we obtain:

$$y_1 = \omega y_1^* \tag{33}$$

with $\omega = (k' K_m D)/(k K'_m A)$. This last result implies that the conservation law for the protein in the upper cycle con be written (neglecting the complexes with the activator and the inactivator, but not those with the downstream targets, and dividing the equation by Y_{1T}) as: $1 = y_1^*(1 + \omega) + c_1 + c_2$, with c_1 and c_2 the normalized complexes with the downstream (double-phosphorylation) cycle. By writing the corresponding equations for c_1 and c_2, solving for the steady-state, and using the previous conservation, we obtain Eq. (18).

References

Alberts B, Johnson A, Lewis J, Raff M, Roberts K (2001) Molecular biology of the cell. Garland Science

Angeli D, Ferrell JE, Sontag ED (2004) Detection of multistability, bifurcations, and hysteresis in a large class of biological positive-feedback systems. Proc Natl Acad Sci USA 101:1822–1827

Bluthgen N, Bruggeman FJ, Legewie S, Herzel H, Westerhoff HV, Kholodenko BN (2006) Detection of multi-stability, bifurcations, and hysteresis in a large class of biological positive-feedback systems. FEBS J 273:895–906

Del Vecchio D, Ninfa AJ, Sontag ED (2008) Modular cell biology: retroactivity and insulation. Mol Syst Biol 4:161

Fages F, Soliman S (2008) In: Lecture notes in computer science, vol 5054. Springer, Berlin

Feliu E, Wiuf C (2012) Enzyme sharing as a cause of multi-stationarity in signaling systems. J R Soc Interface, 9(71):1224–1232
Goldbeter A, Koshland J, DE (1981) An amplified sensitivity arising from covalent modification in biological systems. Proc Natl Acad Sci USA 78(11):6840–6844
Gonze D, Goldbeter A (2001) A model for a network of phosphorylation-dephosphorylation cycles displaying the dynamics of dominoes and clocks. J Theor Biol 210:167–186
Gouzé J (1998) Positive and negative circuits in dynamical systems. J Biol Syst 6(1):11–15
Gross T, Feudel U (2006) Generalized models as an universal approach to the analysis of nonlinear dynamical systems. Phys Rev E 73:016205–016214
Huang CY, Ferrell J, JE (1996) Ultrasensitivity in themitogen-activated protein kinase cascade. Proc Natl Acad Sci USA 93(19):10078–10083
Jiang P, Ventura AC, Sontag ED, Merajver SD, Ninfa AJ, Del Vecchio D (2011) Load-induced modulation of signal transduction networks. Sci Signal 4(194):1–10
Kholodenko B (2000) Negative feedback and ultrasensitivity can bring about oscillations in the mitogen-activated protein kinase cascades. Eur J Biochem 267:1583–1588
Kim Y, Paroush Z, Nairz K, Hafen E, Jimenez G, Shvartsman SY (2011) Substrate-dependent control of mapk phosphorylation *in vivo* Mol Syst Biol 7:467
Markevich NI, Hoek JB, Kholodenko BN (2004) Signaling switches and bistability arising from multisite phosphorylation in protein kinase cascades. J Cell Biol 164:353–359
Murray J (2002) Mathematical biology i : an introduction. 3rd edn. Springer, Berlin
Murray AW, Kirschner MW (1989) Dominoes and clocks: the union of two views of the cell cycle. Science 246:614–621
Ortega F, Acerenza L, Westerhoff HV, Mas F, Cascante M (2002) Product dependence and bifunctionality compromise the ultrasensitivity of signal transduction cascades. Proc Natl Acad Sci USA 99:1170–1175
Ortega F, Garces JL, Mas F, Kholodenko BN, Cascante M (2006) Bistability from double phosphorylation in signal transduction. Kinetic and structural requirements. FEBS J. 273:3915–3926
Ossareh HR, Ventura AC, Merajver SD, Del Vecchio D (2011) Long signaling cascades tend to attenuate retroactivity. Biophys J 100(7):1617–1626
Qiao L, Nachbar RB, Kevrekidis IG, Shvartsman SY (2007) Bistability and oscillations in the huang-ferrell model of mapk signaling. PLoS Comput Biol 3(9):1819–1826
Snoussi E, Thomas R (1993) Logical identi cation of all steady states: the concept of feedback loop characterisitic states. Bull Math Biol 55(5):973–991
Thalhauser C, Komarova N (2010) Signal response sensitivity in the yeast mitogen-activated protein kinase cascade. PLoS One 5(7) doi:10.1371/journal.pone.0011568
Thattai M, van Oudenaarden A (2002) At-tenuation of noise in ultrasensitive signaling cascades. Biophys J 82:2943–2950
Thomas R, D'Ari R (1990) Biological Feedback. CRC Press, Boca Raton
Ventura AC, Sepulchre JA, Merajver SD (2008) A hidden feedback in signaling cascades is revealed. PLoS Comput Biol 4(3):e1000041
Ventura A, Jackson T, Merajver S (2009) On the role of cell signaling models in cancer research. Cancer Res. 69:400–402
Ventura AC, Jiang P, Van Wassenhove L, Del Vecchio D, Merajver SD, Ninfa AJ (2010) Signaling properties of a covalent modification cycle are altered by a downstream target. Proc Natl Acad Sci U S A 107(22):10032–10037
Wagner E, Nebreda A (2009) Signal integration by jnk and p38 mapk pathways in cancer development. Nat Rev Cancer 9:537–549
Wynn ML, Ventura AC, Sepulchre JA, Garcia HJ, Merajver SD (2011) Kinase inhibitors can produce off-target effects and activate linked pathways by retroactivity. BMC Syst Biol 5:156
Zumsande M, Gross T (2010) Bifurcations and chaos in the mapk signaling cascade. J Theor Biol 265:481–491